NEW DIFFRACTION DATA

Synthesis, powder diffraction pattern, crystal structure determination of the pharmaceutical co-crystal of levetiracetam and 3,5-dinitrosalicylic acid

Lingling Shi [ORCID],[1] Zhengguo Chen,[1] Hany Kafafy,[2] Zhaoxia Zhang,[1] Guocheng Zhu,[1] Juming Yao,[1] and Guoqing Zhang[1,a]

[1]*School of Materials Science and Engineering, Zhejiang Sci-Tech University, Hangzhou 310018, People's Republic of China*
[2]*Dyeing, Printing and Auxiliaries Department, Textile Research Division, National Research Center, 33 El-Buhoth St, Dokki, Cairo 12311, Egypt*

(S)-α-Ethyl-2-oxo-1-pyrrolidineacetamide (trade name levetiracetam), a derivative of piracetam, is used clinically as an add-on treatment for partial-onset seizures. In this study, we report the solid-state structure of a new drug co-crystal produced from levetiracetam and 3,5-dinitrosalicylic acid through cooling crystallization. This compound was further characterized by infrared spectroscopy, powder X-ray diffraction, and single-crystal X-ray diffraction. The new co-crystals show a 1:1 stoichiometry and crystallize in the monoclinic system, space group $P2_1$, with cell parameters: $a = 9.7709(3)$ Å, $b = 6.2202(2)$ Å, $c = 14.7280(4)$ Å, $\alpha = 90°$, $\beta = 96.0340(10)°$, $\gamma = 90°$, $V = 890.16(5)$ Å^3, and $Z = 2$. It is identified that hydrogen bonds are the main interactions between levetiracetam and 3,5-dinitrosalicylic acid, and the contribution of each hydrogen bond in maintaining the stability of the crystal structure was also quantified using Hirshfeld surface analysis.

I. INTRODUCTION

Pharmaceutical co-crystal (El-Gizawy et al., 2015; Ervasti et al., 2015) is an application of the concept of supramolecular chemistry in the pharmaceutical industry (Bolla and Nangia, 2016), which consists of active pharmaceutical ingredient (API) and co-crystal formers (CCF) bonded by non-covalent bonds (including hydrogen bonding, van der Waals forces, π-π stacking effects, etc.). Due to their unique physicochemical properties, co-crystals are often used as a new solid form to improve the physicochemical properties of drugs, such as solubility (Ranjan et al., 2017), dissolution rate (Yamashita and Sun, 2018), bioavailability (Yoshimura et al., 2017; Emami et al., 2018), hygroscopicity (Sopyan et al., 2017), and chemical stability (Duggirala et al., 2018). Thus, co-crystals are of extraordinary value for research in the direction of drugs. In fact, co-crystal drugs do not need to go through phase II approval in the clinic research because they are not considered as a new molecular entity, which will save a lot in terms of development costs.

Levetiracetam (LEV) is a pyrrolidone compound, chemically named (S)-α-ethyl-2-oxo-1-pyrrolidineacetamide as a new antiepileptic drug (Zhang et al., 2010; Weijenberg et al., 2015). After extensive research, it was approved by the U.S. FDA in 1999 for the treatment of seizures and finally marketed as a second-generation antiepileptic drug. Levetiracetam is a safer drug for clinical use due to its high bioavailability, linear pharmacokinetics, low protein binding rate, minimal hepatic metabolism, rapid acquisition of stable blood concentrations, and minimal drug interactions.

Levetiracetam molecule contains amine and carbonyl groups (Figure 1(a)), which can act as donors or acceptors of hydrogen bonds, forming coordination compounds with some inorganic salts or organic acids. As a result, co-crystals can form easily through these interactions, further improving the physicochemical properties of levetiracetam. For example, Song et al. (2019) prepared ionic co-crystals of levetiracetam with $CaCl_2$ and $MgCl_2$, successfully improving the thermal stability of levetiracetam (Song et al., 2019).

Organic acids are commonly used as co-crystal formers in drug research and development. Among them, 3,5-dinitrosalicylic acid (abbreviated DNS or DNSA, IUPAC name 2-hydroxy-3,5-dinitrobenzoic acid) as an aromatic acid can easily combine with compounds of various structures to form co-crystals (Figure 1(b)). Its carboxyl group can participate in various O–H···X hydrogen bonds for the formation of monoanionic dimer/trimer of 3,5-dinitrosalicylic acid (D'Ascenzo and Auffinger, 2015).

In this paper, 3,5-dinitrosalicylic acid as a co-crystal former is selected to combine with levetiracetam by non-covalent hydrogen bonds. The co-crystal was first prepared by the cooling crystallization method (Friscic and Jones, 2009) as shown in Scheme 3 of Figure 1(c). To further understand the conformation of the co-crystal of levetiracetam and 3,5-dinitrosalicylic acid, the crystal products were characterized by FTIR spectroscopy, powder X-ray diffraction, and X-ray single-crystal diffraction. In addition, the role of

---

a)Author to whom correspondence should be addressed. Electronic mail: zgq@zstu.edu.cn
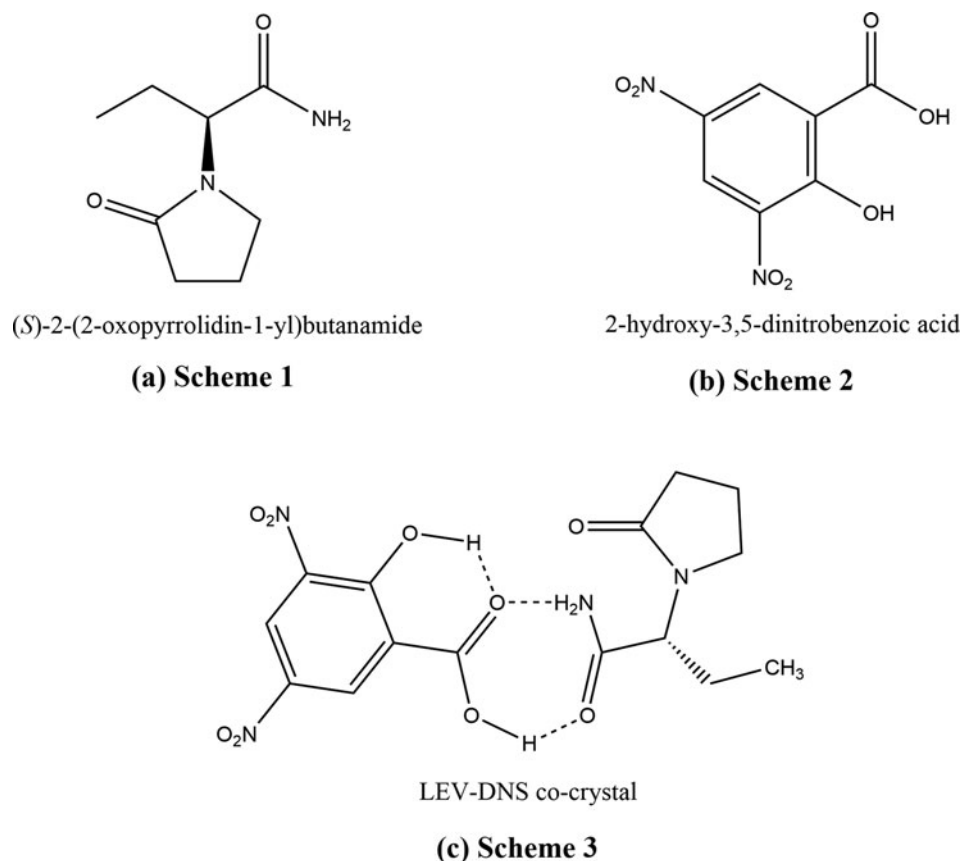
Figure 1. (a) Levetiracetam molecule containing amine and carbonyl groups; (b) 3,5-dinitrosalicylic acid (abbreviated DNS or DNSA, IUPAC name 2-hydroxy-3,5-dinitrobenzoic acid), an aromatic acid combined with compounds of various structures to form co-crystals; and (c) the LEV-DNS co-crystal prepared by the cooling crystallization method.

hydrogen bond was also quantified by Hirshfeld surface analysis (Spackman and Mckinnon, 2002; Clausen et al., 2010; Seth et al., 2011a).

II. EXPERIMENTAL AND REFINEMENT

A. Sample preparations

The drug co-crystals were prepared by mixing levetiracetam and 3,5-dinitrosalicylic acid in a 1:1 molar ratio in pure water. The mixture was heated between 60 and 70 °C under stirring until completely dissolved. After 1 h, the solution was allowed to cool down slowly to room temperature until a large number of bright yellow precipitates formed. The precipitate was filtered and dried to obtain bright yellow co-crystal powder.

To obtain single crystals, 10 mg of the powder was put into a sample bottle containing 30 ml of methyl tert-butyl ether solvent. The mixture solution was shaken until completely dissolved and clear, and then placed in a dry and ventilated place for about a week. One can see that some yellowish crystals will gradually grow up with evaporation of methyl tert-butyl ether, subsequently a small amount of n-heptane as antisolvent was added into the bottle for storage of the crystals.

B. FTIR spectroscopy

The molecular structures of levetiracetam, 3,5-dinitrosalicylic acid, and the synthesized co-crystalline powder were determined by FTIR spectroscopy. All the powder samples were mixed and ground with KBr in a volume ratio of 1:100, respectively, then tested in a wave number range of 500 to 4000 cm^{-1} with a resolution of 4 cm^{-1} and a scan number of 32.

C. Powder X-ray diffraction (PXRD)

X-ray powder diffraction patterns were collected on a D8 Advance diffractometer (Bruker, Germany) under the condition of Cu $K\alpha_1$ radiation ($\lambda = 1.5406$ Å). The tube voltage and current were set at 40 kV and 40 mA, respectively. The 1D detector was employed to collect XRD data over the 2θ range from 5° to 50° with a step size of 0.02° and a counting time of 0.2 s per step. By comparing the powder diffractograms of the API, co-former and co-crystal, it can be determined whether a new crystalline phase has formed.

D. Single-crystal X-ray diffraction and refinement

The block-shaped single crystals of LEV-DNS co-crystal were first obtained by recrystallization from methyl tert-butyl ether solution. A suitable crystal ($0.49 \times 0.23 \times 0.15$ mm^3) was selected and mounted on a glass fiber support on a Bruker APEX-II CCD diffractometer. The crystal was kept at a steady $T = 170$ K during data collection.

The crystal data and structure refinement details are summarized in Table II. All non-hydrogen atoms were refined with anisotropic displacement parameters. All hydrogen atoms bound to carbon atoms are geometrically placed and refined,
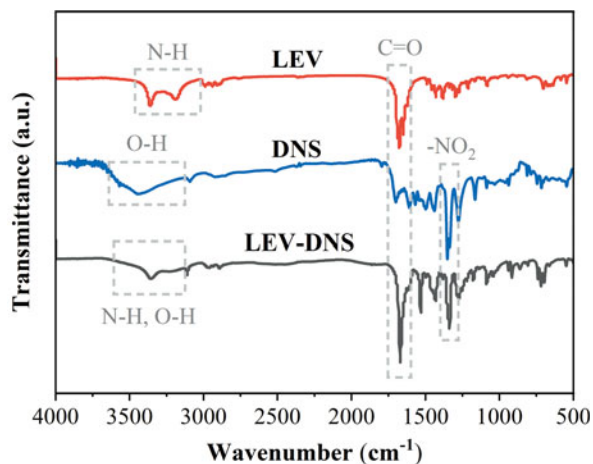
Determination of the pharmaceutical corystal of levetiracetam and 3,5initrosalicylic acid

Figure 2. FTIR spectra of the levetiracetam (LEV), the 3,5-dinitrosalicylic acid (DNS) and the LEV-DNS co-crystal.

= 1.5 U_{eq}(O). The O5–H5A distance of the carboxyl was restrained to 0.84 Å. Other H atoms were generated geometrically and refined using a riding model with hypomethyl C–H = 1.00 Å, U_{iso}(H) = 1.2 U_{eq}(C), methylene C–H = 0.99 Å, aromatic C–H = 0.95 Å, and U_{iso}(H) = 1.2 U_{eq}(C).

III. RESULTS AND DISCUSSION

A. FTIR spectroscopy

FTIR spectroscopy has long been associated with the study of molecular vibrational properties, particularly in relation to the different functional groups present in drugs. The hydrogen bond caused by phase change is directly related to the transformation of the vibration frequency of functional groups. That is the fundamental reason why FTIR can be employed to characterize the co-crystal (Kang et al., 2017; Lin, 2017). In this study, from the FTIR spectra of the two raw materials and the co-crystal (Figure 2), one can see that pure LEV shows two characteristic bands at 3360 and 3192 cm^{-1} corresponding to the symmetric and asymmetric stretching vibrations of N–H in the amide group, respectively. Unlike LEV, DNS shows a wide band between 3640 and 3200 cm^{-1}, which is the result of tensile vibrations of O–H on its phenol and carboxyl groups under the influence of hydrogen bonds. In the FTIR spectrum of the

and their isotropic displacement parameters are derived from the C atoms to which they are attached. The U_{iso}(H) values of all CH$_2$ and CH$_3$ groups were fixed to 1.2 and 1.5 times the U_{eq} values of the attached C atoms, respectively. Similarly, the hydrogen atoms on the amino and hydroxyl groups were refined and optimized with isotropic displacement parameters based on U_{iso}(H) = 1.2 U_{eq}(N) and U_{iso}(H)
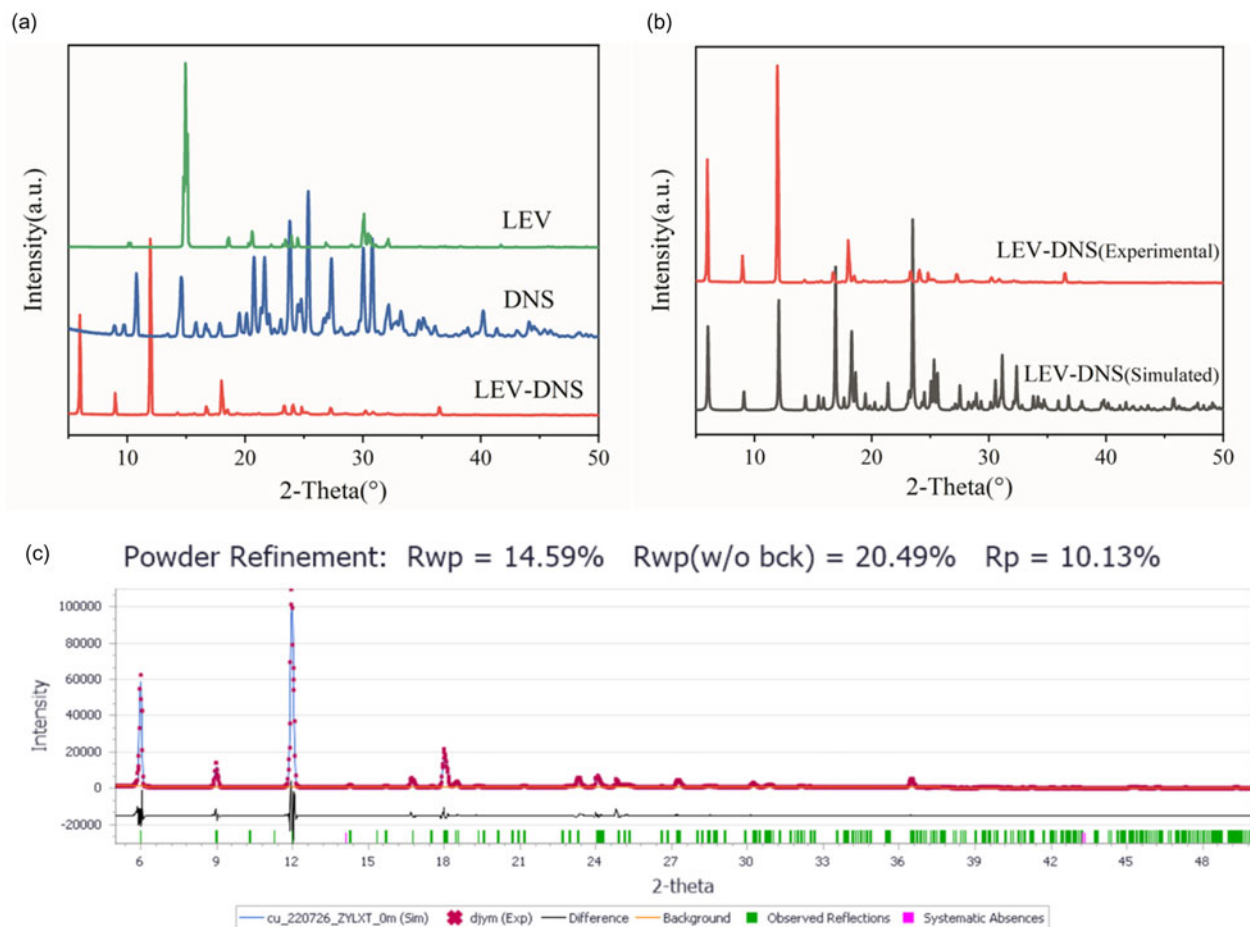

Figure 3. (a) The PXRD patterns of LEV, DNS, and LEV-DNS co-crystal, (b) experimental and simulated XRD patterns of LEV-DNS co-crystal, and (c) Pawley refinement results.

LEV-DNS co-crystal, the N–H stretching vibration peak keeps essentially the same but the O–H stretching vibration peak almost disappears because of the formation of O–H⋯O hydrogen bonds. On the other hand, the absorption peak of the C=O group is red-shifted from 1680 cm^{-1} in LEV and 1700 cm^{-1} in DNS to 1670 cm^{-1}, which is also due to the O–H⋯O hydrogen bonds between the C=O group and the ligand molecule, resulting in a decrease in the vibrational frequency of the carbonyl group and hence a blue-shift of the characteristic peak. This also shows that the carboxylic acid group remains neutral in the product of the reaction of LEV with DNS (Xu et al., 2014). Similarly, both DNS and LEV-DNS co-crystals show a characteristic peak belonging to nitro (–NO$_2$) at 1337 cm^{-1}, indicating that nitro is not involved in the reaction. Therefore, the FTIR data confirm that the co-crystals are indeed formed as suggested in Figure 2.

B. Powder X-ray diffraction (PXRD)

The PXRD pattern of a crystalline sample is considered as the fingerprint of its crystal structure. Every crystalline material will exhibit unique peaks indicative of diffraction from specific atomic planes (Newman and Byrn, 2003). The XRD patterns of levetiracetam (LEV), 3,5-dinitrosalicylic acid (DNS), and their co-crystal products (LEV-DNS) are shown in Figure 3(a).

As can be seen from the figure, the strong characteristic peaks are observed at 2θ 14.970°, 20.576°, and 30.102° for the LEV, while the peaks for DNS appear at 2θ 10.871°, 14.684°, and 21.679°. On the other hand, the strong characteristic peaks for the LEV-DNS co-crystal appear at 2θ 6.020°, 11.954°, and 17.989° which is completely different from the precursors. It is thus clear that the co-crystal product is not a simple physical mixing of the two raw materials, but indeed a new crystalline phase. Furthermore, from

TABLE I. X-ray powder diffraction data of LEV-DNS co-crystal before and after Pawley refinement.

2θ_{obs} (°)	d_{obs} (Å)	$(I/I_o)_{obs}$	h	k	l	2θ_{cal} (°)	d_{cal} (Å)	$(I/I_o)_{cal}$	$\Delta 2\theta$ (°)
5.980	14.7674	56.2	0	0	1	5.981	14.6514	44	0.001
8.962	9.8596	12.2	1	0	0	8.987	9.7494	10.6	0.025
11.234	7.8697	0.2	1	0	1	11.275	7.7746	0.2	0.041
11.954	7.3972	100	0	0	2	11.967	7.3257	100	0.013
14.279	6.1976	1.2	1	0	−2	14.261	6.1518	1.3	−0.018
15.318	5.7794	0.4	0	1	1	15.325	5.7271	0.5	0.007
15.666	5.6518	0.7	1	0	2	15.674	5.6003	0.9	0.008
16.704	5.3029	4.7	1	1	0	16.743	5.2450	6.2	0.039
17.501	5.0632	0.4	1	1	−1	17.491	5.0224	0.6	−0.010
17.992	4.9260	19.4	0	0	3	17.991	4.8838	10.5	−0.001
18.518	4.7875	2.9	2	0	−1	18.437	4.7667	2.4	−0.081
19.315	4.5915	0.8	1	0	−3	19.333	4.5477	1.1	0.018
19.559	4.5349	0.4	2	0	1	19.558	4.4960	0.5	−0.001
20.133	4.4069	0.2	1	1	−2	20.107	4.3746	0.2	−0.026
20.738	4.2797	0.3	2	0	−2	20.683	4.2541	0.3	−0.055
21.170	4.1933	0.7	1	1	2	21.143	4.1625	0.9	−0.027
22.985	3.8662	0.7	2	1	0	22.960	3.8373	1	−0.025
23.331	3.8096	4.8	2	1	−1	23.289	3.7840	6.5	−0.042
24.065	3.6949	5.5	0	0	4	24.071	3.6628	6.7	0.006
24.805	3.5864	4.2	1	0	−4	24.888	3.5445	2.7	0.083
25.189	3.5326	1.3	2	1	−2	25.124	3.5118	1.3	−0.065
26.610	3.3470	0.3	1	0	4	26.572	3.3238	0.2	−0.038
26.859	3.3166	0.3	2	0	3	26.823	3.2933	0.3	−0.036
27.230	3.2722	3.6	3	0	−1	27.272	3.2402	4.6	0.042
28.082	3.1748	0.2	0	1	4	28.010	3.1565	0.2	−0.072
28.531	3.1260	0.7	0	2	0	28.429	3.1111	0.9	−0.102
28.753	3.1023	0.3	2	0	−4	28.761	3.0759	0.2	0.008
29.780	2.9976	0.2	1	2	0	29.875	2.9638	0.3	0.095
30.225	2.9545	2.2	1	1	4	30.211	2.9317	2.8	−0.014
30.877	2.8936	1.3	3	1	−1	30.835	2.8739	1.1	−0.042
31.734	2.8173	0.2	2	0	4	31.670	2.8001	0.3	−0.064
32.160	2.7810	0.7	2	1	−4	32.175	2.7574	0.6	0.015
32.447	2.7571	0.5	1	0	5	32.461	2.7337	0.5	0.014
33.488	2.6737	0.2	0	1	5	33.506	2.6510	0.3	0.018
34.016	2.6334	0.2	2	0	−5	33.821	2.6271	0.1	−0.195
34.563	2.5929	0.2	3	1	−3	34.450	2.5807	0.3	−0.113
35.624	2.5181	0.2	1	2	3	35.585	2.5011	0.3	−0.039
36.484	2.4607	4.4	0	0	6	36.480	2.4419	4.4	−0.004
37.673	2.3858	0.3	4	0	1	37.676	2.3672	0.2	0.003
39.527	2.2780	0.4	1	1	−6	39.550	2.2596	0.3	0.023
39.922	2.2563	0.2	3	2	−1	39.835	2.2441	0.2	−0.087
41.258	2.1863	0.1	1	1	6	41.249	2.1706	0.1	−0.009
45.332	1.9989	0.2	0	1	7	45.354	1.9838	0.2	0.022
46.194	1.9636	0.2	5	0	0	46.192	1.9499	0.2	−0.002
49.311	1.8465	0.2	4	2	−3	49.302	1.8343	0.1	−0.009

Determination of the pharmaceutical corystal of levetiracetam and 3,5initrosalicylic acid

Crystal data	
Chemical formula	$C_{15}H_{18}N_4O_9$
M_r	398.33
Crystal system, space group	Monoclinic, $P2_1$
a, b, c (Å)	9.7709(3), 6.2202(2), 14.7280(4)
α, β, γ (°)	90, 96.0340(10), 90
V (Å^3)	890.16(5)
Z	2
Radiation type	Cu $K\alpha$
μ (mm^{-1})	1.076
Crystal size (mm)	$0.49 \times 0.23 \times 0.15$
Data collection	
Diffractometer	Bruker APEX-II CCD
T_{min}, T_{max} (°)	0.597, 0.753
No. of measured, independent and observed [$I > 2\sigma(I)$] reflections	12,414, 3174, 3169
R_{int}	0.0219
$(\sin \theta/\lambda)$max (Å^{-1})	0.648
Refinement	
$R[F^2 > 2\sigma(F^2)]$, $wR(F^2)$, S	0.0267, 0.0720, 1.062
No. of reflections	3174
No. of parameters	258
No. of restraints	2
H-atom treatment	H-atoms treated by a mixture of independent and constrained refinement
$\Delta\rho_{max}, \Delta\rho_{min}$ (e Å^{-3})	0.19, −0.17
Absolute structure	Flack x determined using 1377 quotients [$(I^+)-(I^-)$]/[$(I^+)+(I^-)$] (Parsons, Flack and Wagner, *Acta Crystallographica* B69 (2013): 249–59).

For the single-crystal structure: monoclinic, $P2_1$, $Z = 2$. Experiments were carried out at 170 K with Cu $K\alpha$ radiation using a Bruker APEX-II CCD diffractometer. Absorption was corrected for by multi-scan methods.

Figure 3(b), the experimental PXRD patterns from the grinding are in general agreement with the simulated patterns calculated from the structural parameters of the present LEV-DNS single crystals. The only difference in the relative intensities of some diffraction peaks can be attributed to changes in crystal habit or crystal size (Pandey et al., 2017), further confirming the crystalline phase purity of the co-crystals (Figure 3(b)).

In order to obtain more accurate results, this paper uses the Reflex module in the Material Studio (Dassault Systèmes, 2021) software to perform Pawley refinement of the powder XRD pattern and then compares it with the simulated XRD
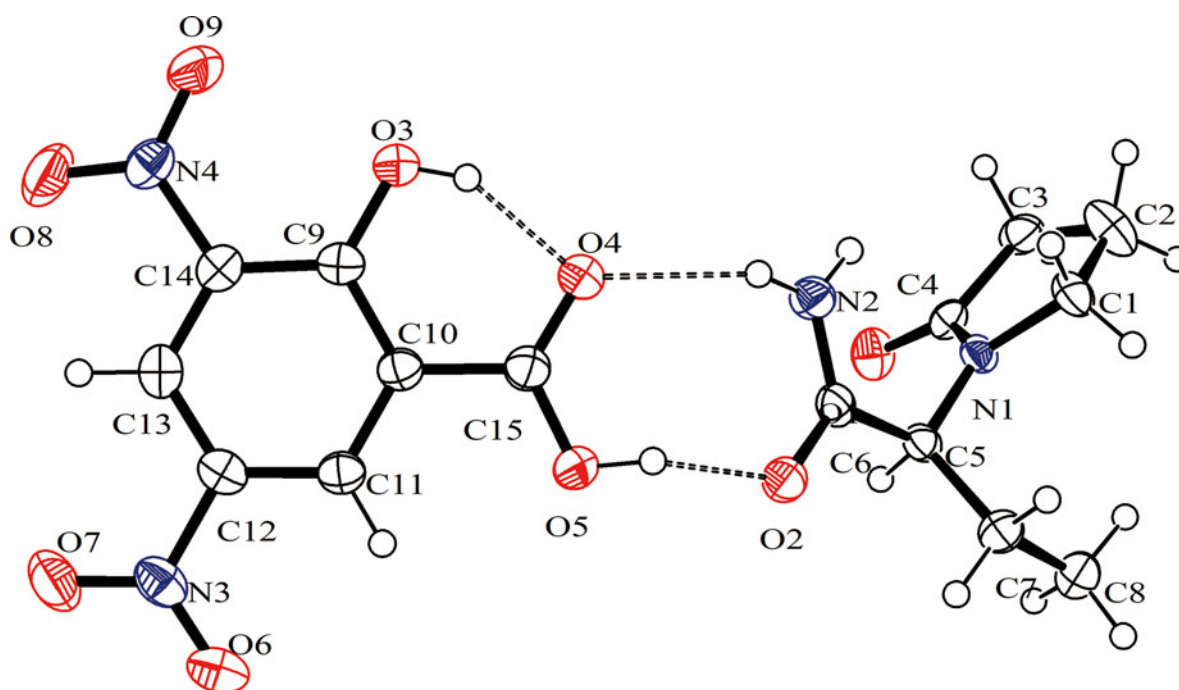

Figure 4.   The molecular structures of LEV-DNS co-crystal show the atom-numbering schemes. Displacement ellipsoids are drawn at the 50% probability level. Dashed lines indicate hydrogen bonds.
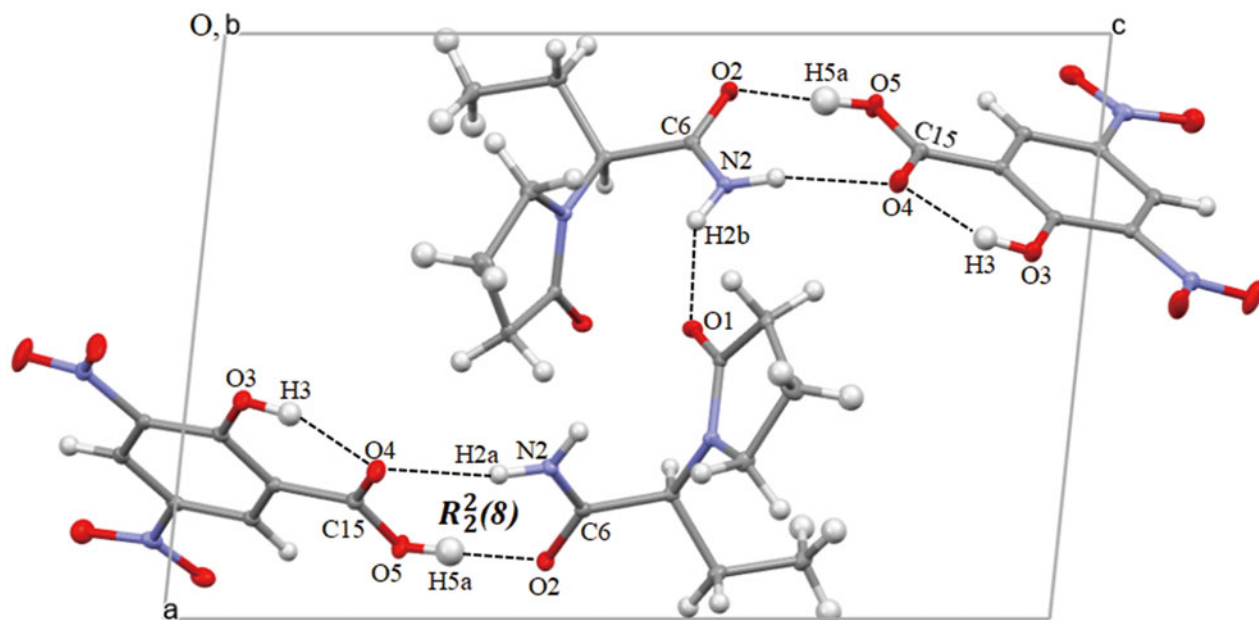
Figure 5. Interactions occurring in the LEV-DNS co-crystal, the dashed lines represent hydrogen bonds.
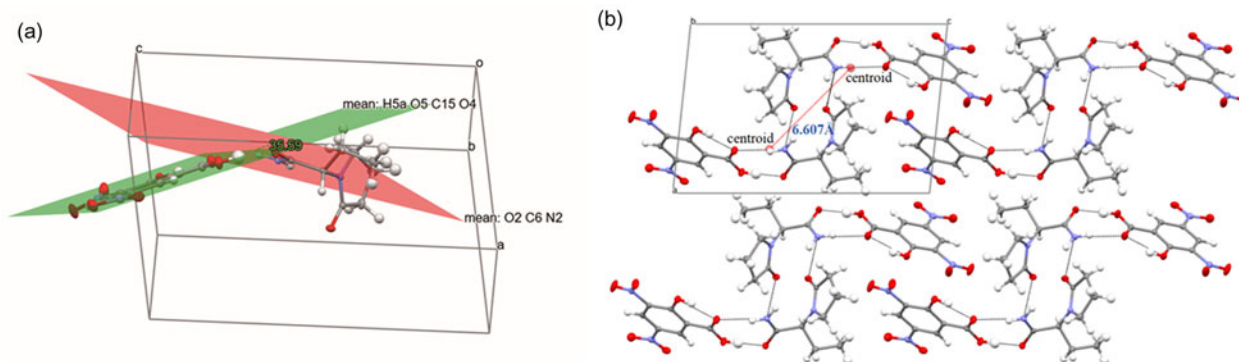

Figure 6. (a) Dihedral angle between LEV molecules and DNS molecules in an asymmetric structural unit and (b) intermolecular interaction diagram of LEV-DNS (along the b-axis).
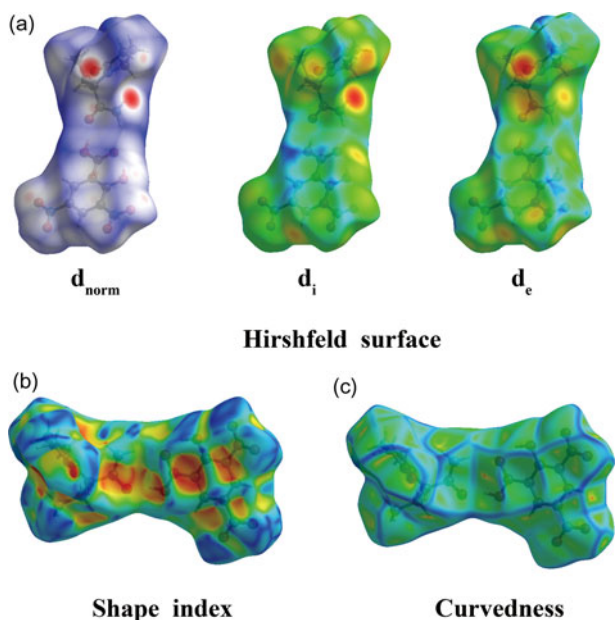

Figure 7. (a) Hirshfeld surface generated over d_{norm}, di and de for LEV-DNS co-crystal; (b) shape index; and (c) curvedness mapped over the Hirshfeld analysis.

data from the single crystals. As shown in Figure 3(c), the Pawley refinement, including the background, zero error, cell parameters, peak width, and peak symmetry parameters, was carried out successfully. The residuals of the final fit, $R_{wp} = 14.59\%$ and $R_p = 10.13\%$, are less than 15%, which is an acceptable error range. The values of $2\theta_{obs}$, d_{obs}, I_{obs}, h, k, l, $2\theta_{cal}$, d_{cal}, I_{cal}, and $\Delta 2\theta$ are listed in Table I.

C. Single-crystal structure

From the single-crystal structure data listed in Table II, it can be seen that the space group of the obtained co-crystal is $P2_1$, belonging to the monoclinic system with cell parameters of $a = 9.7709(3)$ Å, $b = 6.2202(2)$ Å, $c = 14.7280(4)$ Å, $\alpha = \gamma$

TABLE III. Hydrogen-bond geometry (Å, °) for LEV-DNS co-crystal.

D-H···A	D-H	H···A	D···A	D-H···A
N2–H2B···O1[i]	0.88	2.02	2.802(2)	147.5
O5–H5A···O2	0.91(2)	1.62(2)	2.501(2)	165(4)
O3–H3···O4	0.84	1.77	2.5250(19)	148.6

Symmetry codes: (i) $1-x$, $-1/2 + y$, $1-z$.

Determination of the pharmaceutical corystal of levetiracetam and 3,5initrosalicylic acid

$= 90°$, and $\beta = 96.0340(10)°$. As a solvent-free compound, each asymmetric unit consists of two molecules of levetiracetam (LEV) and two molecules of 3,5-dinitrosalicylic acid (DNS) in a 1:1 ratio. There is no proton transfer between the LEV and DNS molecules, but linked together by hydrogen bonds to form a heterodimeric structure (Figure 4). In this dimer, the two DNS molecules are connected by a hydrogen bond N2–H2b⋯O1. DNS is linked to the LEV molecule through two hydrogen bonds, O5–H5A⋯O2 and O3–H3⋯O4, being represented by the graph set symbol as $R_2^2(8)$ (Figure 5). The hydrogen bonding details and symmetry codes of the LEV-DNS co-crystal are given in Table III.

In fact, the co-crystals formed by levetiracetam and 3,5-dinitrosalicylic acid are not coplanar, and the angle between the two planes formed by the connection of the two molecules is 35.59° (Figure 6(a)). The co-crystal's molecular arrangement, driven by hydrogen bonding, becomes apparent along the b-axis, resulting in the creation of a double-layered, one-dimensional chain reminiscent of the mathematical concept of an open root "$\sqrt{\ }$" (Figure 6(b)), with a distance of
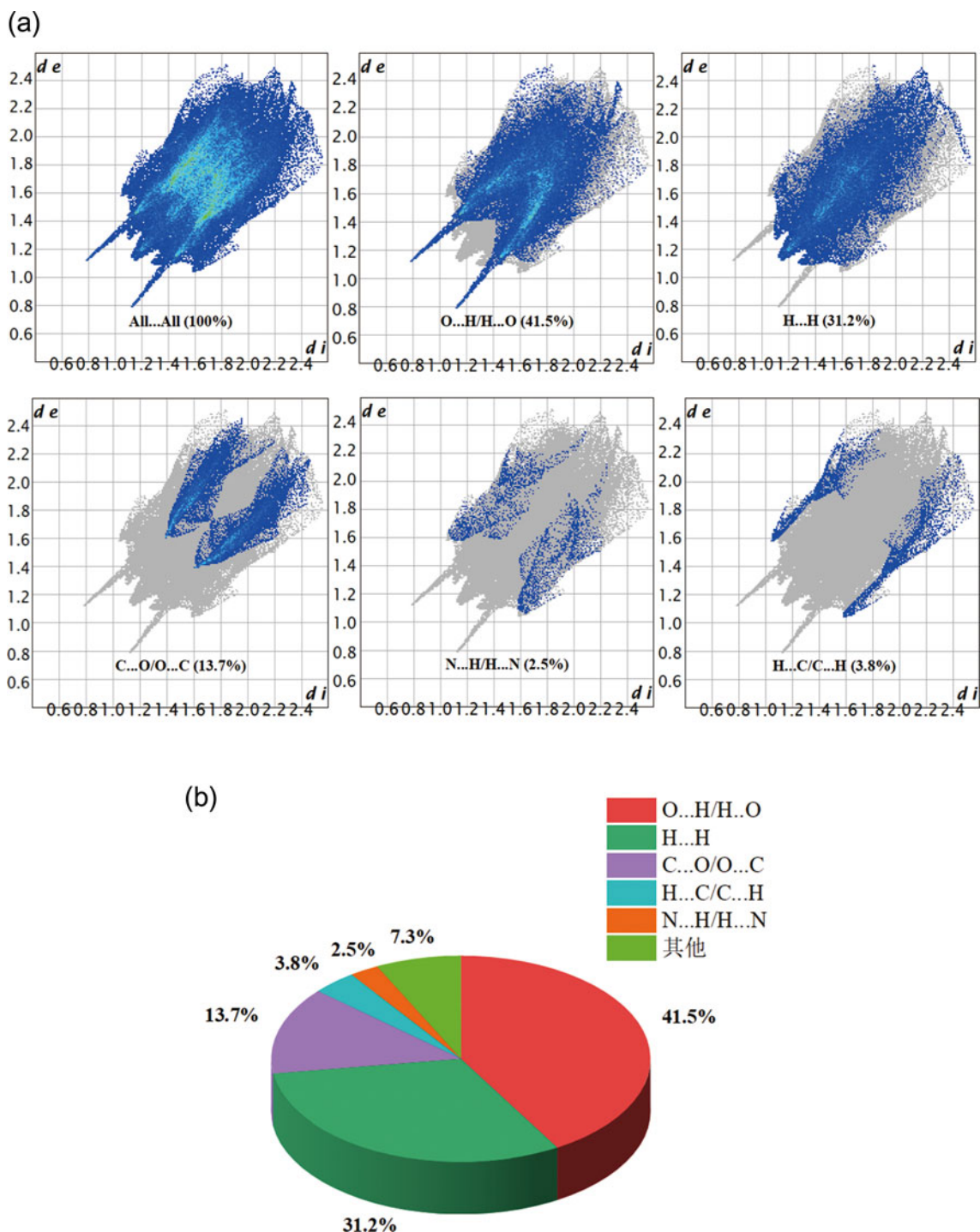

Figure 8. (a) The 2D fingerprint plot of various intermolecular interaction forces and (b) Pie chart of the relative contribution of various intermolecular interactions on the Hirshfeld surface.

6.607 Å between the two co-crystal molecules in the one-dimensional chain.

D. Hirshfeld surface analysis

The intermolecular interactions of the LEV-DNS co-crystal were also studied in a targeted and visualized manner by CrystalExplorer software (Spackman et al., 2021). Figure 7(a) shows the Hirshfeld surfaces of the LEV-DNS co-crystal, where d_i is the shortest distance from the Hirshfeld surface to the inner atom and d_e is the shortest distance from the Hirshfeld surface to the outer atom (Spackman and Jayatilaka, 2009), and d_{norm} is the surface map which depicts the individual hydrogen bonding interactions on the d_{norm} surface. The 3D d_{norm} surface is usually used to identify closer intermolecular interactions by taking into account the relative size of the atoms. In general, these are shown as red areas (relatively strong forces appearing as bright red or light red round spots) on the Hirshfeld surface when the length of the intermolecular interaction is shorter than r^{vdw} (van der Waals (vdw) radius), conversely in white or blue when equal to or greater than r^{vdw}.

The shape index represents the bumps (blue) and hollows (red) presented in the system (Figure 7(b)). It is clear that the crystal structure of the LEV-DNS does not exhibit any $\pi . . . \pi$ stacking interaction since there is no evidence of the adjacent red and blue triangles on the shape index surface (Seth et al., 2011b). In addition, the curvedness in the crystal structure shows the stacking of molecules in 3D space based on the presence of a flat green region (Figure 7(c); Soman et al., 2014).

The 2D fingerprint plots of intermolecular interactions reflect the way in which molecules interact within a structure and the extent to which each type of interaction contributes to the overall effect (Nikpour et al., 2009). As shown in Figure 8 (a), the O···H/O···H intermolecular interactions exhibit a pair of symmetrical large spikes, characteristic of strong hydrogen bonding, and these interactions account for 41.5% of the total Hirshfeld surface area. H···H interactions also characterize a significant contribution to the Hirshfeld surface, accounting for 31.2% of the total surface area. Interactions between LEV-DNS co-crystals also include C···O/O···C interactions, but they do not dominate the crystal structure, accounting for only 13.7% of the total surface area. In addition, C···H/H···C and N···H/H···N interactions were present on only 3.8 and 2.5% of the total surface area, respectively (Figure 8 (b)). It is clear that O–H···O hydrogen bonding is the major contributor to the interactions in this structure.

IV. CONCLUSION

Although the antiepileptic drug levetiracetam has been available for many years, there is still relatively little information on its crystallographic aspects. In this paper, co-crystals of 3,5-dinitrosalicylic acid and levetiracetam were obtained by cooling (powder crystals) and solvent evaporation (single crystals) crystallization, subsequently a series of structural characterizations were carried out and analyzed.

The powder product formed after cooling crystallization can be identified by FTIR spectroscopy and X-ray diffraction, indicating the formation of the co-crystals. The single-crystal structure analysis reveals that the co-crystals of levetiracetam and 3,5-dinitrosalicylic acid are classified within the monoclinic crystal system, characterized by the $P2_1$ space group. These co-crystals are intricately connected through intermolecular hydrogen bonding forces, resulting in the formation of a distinctive structural motif. Specifically, these hydrogen bonding interactions give rise to a double layer of one-dimensional chains, adopting a unique shape resembling "$\sqrt{}$". In addition, the Hirshfeld surface analysis and 2D fingerprints about LEV-DNS co-crystal reveal the degree of contribution of various intermolecular interaction forces. It is clear that the intermolecular hydrogen bonding forces are the main contributor to the overall interaction forces.

V. DEPOSITED DATA

The Crystallographic Information System file $C_8H_{14}N_2O \cdot C_7H_4N_2O_7$ co-crystal cif (for the single-crystal data) were deposited with the ICDD. The data files can be requested at pdj@icdd.com.

Supplementary material

The supplementary material for this article can be found at https://doi.org/10.1017/S0885715623000374.

Funding statement

Conflict of interest

The authors have no conflict of interest to declare.

REFERENCES

Bolla, G., and A. Nangia. 2016. "Pharmaceutical Cocrystals: Walking the Talk." *Chemical Communications* 52 (54): 8342–60.

Clausen, H. F., M. S. Chevallier, M. A. Spackman, and B. B. Iversen. 2010. "Three New Co-Crystals of Hydroquinone: Crystal Structures and Hirshfeld Surface Analysis of Intermolecular Interactions." *New Journal of Chemistry* 34 (2): 193–99.

D'Ascenzo, L., and P. Auffinger. 2015. "A Comprehensive Classification and Nomenclature of Carboxyl–Carboxyl (ate) Supramolecular Motifs and Related Catemers: Implications for Biomolecular Systems." *Acta Crystallographica Section B: Structural Science, Crystal Engineering and Materials* 71 (2): 164–75.

Dassault Systèmes. 2021. *Materials Studio. V. 2021*. BIOVIA. Windows.

Duggirala, N. K., H. L. Frericks Schmidt, Z. Lei, M. J. Zaworotko, J. F. Krzyzaniak, and K. K. Arora. 2018. "Solid-State Characterization and Relative Formation Enthalpies to Evaluate Stability of Cocrystals of an Antidiabetic Drug." *Molecular Pharmaceutics* 15 (5): 1901–08.

El-Gizawy, S. A., M. A. Osman, M. F. Arafa, and G. M. El Maghraby. 2015. "Aerosil as a Novel Co-Crystal Co-Former for Improving the Dissolution Rate of Hydrochlorothiazide." *International Journal of Pharmaceutics* 478 (2): 773–78.

Emami, S., M. Siahi-Shadbad, K. Adibkia, and M. Barzegar-Jalali. 2018. "Recent Advances in Improving Oral Drug Bioavailability by Cocrystals." *Bioimpacts* 8 (4): 305–20.

Ervasti, T., J. Aaltonen, and J. Ketolainen. 2015. "Theophylline–Nicotinamide Cocrystal Formation in Physical Mixture During Storage." *International Journal of Pharmaceutics* 486 (1–2): 121–30.

Friscic, T., and W. Jones. 2009. "Recent Advances in Understanding the Mechanism of Cocrystal Formation via Grinding." *Crystal Growth and Design* 9 (3): 1621–37.

Kang, Y., J. Gu, and X. Hu. 2017. "Syntheses, Structure Characterization and Dissolution of Two Novel Cocrystals of Febuxostat." *Journal of Molecular Structure* 1130: 480–86.

Lin, S. Y. 2017. "Simultaneous Screening and Detection of Pharmaceutical Co-Crystals by the One-Step DSC–FTIR Microspectroscopic Technique." *Drug Discovery Today* 22 (4): 718–28.

Newman, A. W., and S. R. Byrn. 2003. "Solid-State Analysis of the Active Pharmaceutical Ingredient in Drug Products." *Drug Discovery Today* 8 (19): 898–905.

Nikpour, M., M. Mirzaei, Y. G. Chen, A. A. Kaju, and M. Bakavoli. 2009. "Contribution of Intermolecular Interactions to Constructing Supramolecular Architecture: Synthesis, Structure and Hirshfeld Surface Analysis of a New Hybrid of Polyoxomolybdate and ((1H-Tetrazole-5-yl) Methyl) Morpholine." *Inorganic Chemistry Communications* 12 (9): 879–82.

Pandey, N. K., H. R. Sehal, V. Garg, T. Gaur, B. Kumar, S. K. Singh, M. Gulati, K. Gowthamarajan, P. Bawa, S. Y. Rajesh, P. Sharma, and R. Narang. 2017. "Stable Co-Crystals of Glipizide with Enhanced Dissolution Profiles: Preparation and Characterization." *Aaps PharmSciTech* 18: 2454–65.

Ranjan, S., R. Devarapalli, S. Kundu, V. R. Vangala, A. Ghosh, and C. M. Reddy. 2017. "Three New Hydrochlorothiazide Cocrystals: Structural Analyses and Solubility Studies." *Journal of Molecular Structure* 1133: 405–10.

Seth, S. K., N. C. Saha, S. Ghosh, and T. Kar. 2011a. "Structural Elucidation and Electronic Properties of Two Pyrazole Derivatives: A Combined X-Ray, Hirshfeld Surface Analyses and Quantum Mechanical Study." *Chemical Physics Letters* 506 (4–6): 309–14.

Seth, S. K., G. C. Maity, and T. Kar. 2011b. "Structural Elucidation, Hirshfeld Surface Analysis and Quantum Mechanical Study of Para-Nitro Benzylidene Methyl Arjunolate." *Journal of Molecular Structure* 1000 (1–3): 120–26.

Soman, R., S. Sujatha, and C. Arunkumar. 2014. "Quantitative Crystal Structure Analysis of Fluorinated Porphyrins." *Journal of Fluorine Chemistry* 163: 16–22.

Song, L., O. Shemchuk, K. Robeyns, D. Braga, F. Grepioni, and T. Leyssens. 2019. "Ionic Cocrystals of Etiracetam and Levetiracetam: The Importance of Chirality for Ionic Cocrystals." *Crystal Growth & Design* 19 (4): 2446–54.

Sopyan, I., A. Fudholi, M. Muchtaridi, and I. P. Sari. 2017. "Simvastatin-Nicotinamide Co-Crystal: Design, Preparation and Preliminary Characterization." *Tropical Journal of Pharmaceutical Research* 16 (2): 297–303.

Spackman, M. A., and D. Jayatilaka. 2009. "Hirshfeld Surface Analysis." *CrystEngComm* 11 (1): 19–32.

Spackman, M. A., and J. J. McKinnon. 2002. "Fingerprinting Intermolecular Interactions in Molecular Crystals." *CrystEngComm* 4 (66): 378–92.

Spackman, P. R., M. J. Turner, J. J. McKinnon, S. K. Wolff, D. J. Grimwood, D. Jayatilaka, and M. A. Spackman. 2021. "Crystalexplorer: A Program for Hirshfeld Surface Analysis, Visualization and Quantitative Analysis of Molecular Crystals." *Journal of Applied Crystallography* 54 (3): 1006–11.

Weijenberg, A., O. F. Brouwer, and P. M. Callenbach. 2015. "Levetiracetam Monotherapy in Children with Epilepsy: A Systematic Review." *CNS Drugs* 29: 371–82.

Xu, Y., L. Jiang, and X. Mei. 2014. "Supramolecular Structures and Physicochemical Properties of Norfloxacin Salts." *Acta Crystallographica Section B: Structural Science, Crystal Engineering and Materials* 70 (4): 750–60.

Yamashita, H., and C. C. Sun. 2018. "Improving Dissolution Rate of Carbamazepine-Glutaric Acid Cocrystal Through Solubilization by Excess Conformer." *Pharmaceutical Research* 35: 1–7.

Yoshimura, M., M. Miyake, T. Kawato, M. Bando, M. Toda, Y. Kato, T. Fukami, and T. Ozeki. 2017. "Impact of the Dissolution Profile of the Cilostazol Cocrystal with Supersaturation on the Oral Bioavailability." *Crystal Growth & Design* 17 (2): 550–57.

Zhang, Y. Q., J. Li, Y. Hu, Y. Tian, and C. H. Gao. 2010. "The Antiepileptic Drug Levetiracetam." *Chinese Journal of Neuroimmunology and Neurology* 17 (2): 145–47.